Communication between the Two Active Sites of Glutathione S-Transferase A1-1, Probed Using Wild-Type−Mutant Heterodimers†

Stephanie A. Misquitta and Roberta F. Colman*

Department of Chemistry and Biochemistry, University of Delaware, Newark, Delaware 19716

Received March 10, 2005; Revised Manuscript Received April 29, 2005

ABSTRACT: To study the communication between the two active sites of dimeric glutathione S-transferase A1-1, we used heterodimers containing one wild-type (WT) active site and one active site with a single mutation at either Tyr9, Arg15, or Arg131. Tyr9 and Arg15 are part of the active site of the same subunit, while Arg131 contributes to the active site of the opposite subunit. The V_{max} values of Tyr9 and Arg15 mutant enzymes were less than 2% that of WT, indicating their importance in catalysis. In contrast, V_{max} values of Arg131 mutant enzymes were about 50−90% of that of WT enzyme while K_m^{GSH} values were approximately 3−8 times that of WT, suggesting that Arg131 plays a role in glutathione binding. The mutant enzyme (with a His_6 tag) and the WT enzyme (without a His_6 tag) were used to construct heterodimers (WT−Y9F, WT−Y9T, WT−R15Q, WT−R131M, WT−R131Q, and WT−R131E) by incubation of a mixture of wild-type and mutant enzyme at pH 7.5 in buffer containing 1,6-hexanediol, followed by dialysis against buffer lacking the organic solvent. The resultant *heterodimers* were separated from the wild-type and mutant *homodimers* using chromatography on nickel-nitrilotriacetic acid agarose. The V_{max} values of all heterodimers were lower than expected for independent active sites. Our experiments demonstrate that mutation of an amino acid residue in one active site affects the activity in the other active site. Modeling studies show that key amino acid residues and water molecules connect the two active sites. This connectivity is responsible for the cross-talk between the active sites.

Glutathione S-transferases (EC 2.5.1.18) (GSTs)[1] are a group of enzymes involved in detoxification mechanisms. They conjugate glutathione to several types of toxic compounds and thus facilitate their removal by degradation within the cell and/or secretion outside the cell. They are also involved in the transport of biological molecules and synthesis of steroid hormones (*1*). GSTs are highly expressed in tumor cells and have been implicated in the development of resistance to anticancer drugs (*2*, *3*). They are also known to modulate the activity of proteins such as Jun N-terminal kinase and apoptosis signal-regulating kinase (*4*, *5*). GSTs therefore play an important role not only in protection of cells but also in other functions as well.

GSTs are grouped into different classes based on their primary structure and substrate specificity (*3*). The GSTs belonging to the alpha class are mainly found in the liver and comprise 2% of the total cystolic protein in this organ (*6*). GSTA1-1 is a homodimer containing two identical active sites per dimer. Each subunit has a glutathione binding site (G-site) and at least one hydrophobic binding site (H-site). The binding sites are located on either side of a V-shaped cleft (Figure 1). Whether the activity in one subunit influences the active site of the other subunit is a question that has been the subject of recent study.

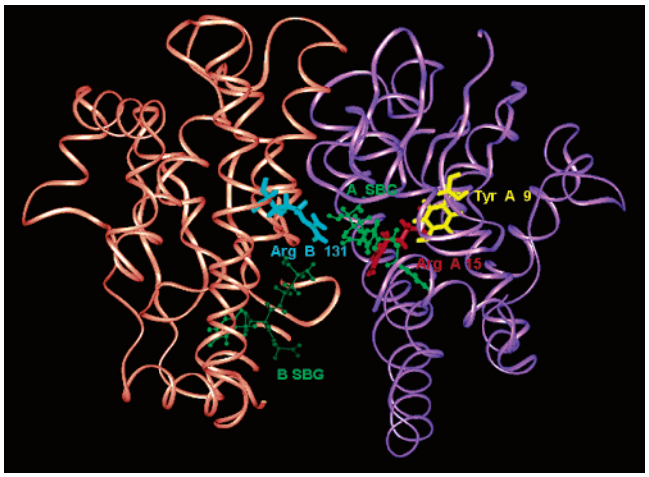

FIGURE 1: Crystal structure of human GSTA1-1 (PDB: 1GUH). The V-shaped cleft between the subunits is clearly visible in this view. The backbone of subunit A is purple, and that of subunit B is orange. The inhibitor, S-benzyl glutathione (SBG), is shown in green, bound in both subunits. Tyr9 (yellow) and Arg15 (red) of subunit A and Arg131 (cyan) of subunit B are residues that were mutated in this study.

Glutathione conjugates are known to bind to GSTA3-3 in a stoichiometric ratio of either 1 or 2 mol/dimer depending on the size of the conjugate (*7*). In the former case, binding of one mole of the conjugate in one active site inhibits binding in the other active site, suggesting that one subunit

† This work was supported by NIH Grant CA-66561.

* To whom correspondence should be addressed. Phone: (302) 831-2973. Fax: (302) 831-6335. E-mail: rfcolman@chem.udel.edu.

[1] Abbreviations: GSTA1-1, glutathione S-transferase from alpha class, isozyme 1-1; WT, wild-type enzyme; GSH, glutathione; CDNB, 1-chloro-2,4-dinitrobenzene; Ni-NTA, nickel-nitrilotriacetic acid agarose; IPTG, isopropyl-β-D-thiogalactoside; EDTA, ethylenediaminetetraacetic acid; PTH, phenylthiohydantoin; SDS−PAGE, sodium dodecyl sulfate−polyacrylamide gel electrophoresis; CD, circular dichroism.

10.1021/bi050449a CCC: $30.25
Published on Web 05/27/2005

affects the function of the other subunit under certain conditions. Affinity labeling of GSTA1-1 at the steroid site resulted in reagent incorporation of only 0.5 mol of reagent/mol of monomer (*8*); and photoaffinity labeling of only one subunit in GSTM2-2[2] and GSTA1-1 caused complete inactivation of the enzyme (*9*, *10*). However, other studies indicate that the two subunits act independently of each other (*11*). Few studies have used mutant enzymes to examine the possibility of subunit−subunit interaction. One such study showed that mutation of Asp101 in one subunit had no effect on the nucleophilic aromatic substitution reaction in the other wild-type subunit (*12*). However, in another study, mutation of residues located at the dimer interface of GSTA1-1 revealed that communication across the interface occurs if unfavorable interactions exist over a short distance (*13*).

In the present study, we evaluate the interaction between the two subunits of GSTA1-1 by mutating amino acid residues that contribute to the active site in the same subunit and compare the results with those involving mutation of a residue contributed to the active site from the other subunit. We considered three residues that have been identified in the crystal structure of GSTA1-1 as active site participants (*14*). Tyr9 and Arg15 are two residues that interact with the substrate in the active site of the same subunit (Figure 1). Tyr9 has been shown to be critical for catalysis (*15*, *16*, *17*) while Arg15 is important for the binding and activation of GSH (*18*, *19*). In contrast, Arg131 is a residue of subunit B which interacts with glutathione bound to the active site of subunit A (Figure 1). We have constructed heterodimers containing one subunit with a wild-type active site and one subunit with a single mutation in the active site; and then investigated the influence of the mutant subunit on the activity of the wild-type subunit. Our experiments indicate that, in all cases, mutation and subsequent loss of activity in one subunit affects the activity in the other wild-type subunit, pointing to communication between the two active sites of the dimer.

EXPERIMENTAL PROCEDURES

*Material*s. Glutathione, 1-chloro-2,4-dinitrobenzene, S-hexylglutathione Sepharose, S-hexylglutathione, imidazole, and chemicals for the preparation of buffers were obtained from Sigma Chemical Co. Nickel-nitrilotriacetic acid agarose (Ni-NTA) was purchased from Qiagen Inc. 1,6-Hexanediol was supplied by ACROS Organics. Primers for mutations were obtained from Biosynthesis Inc. Reagents used for mutagenesis were from Stratagene. The kit used for plasmid extraction was from Qiagen Inc. The Bio-Rad dye reagent for protein estimation was provided by Bio-Rad Laboratories. Amicon Ultra-15 concentrators were from Millipore. All chemicals were of reagent grade.

Mutagenesis and Expression of Protein. The full-length cDNA for rat GSTA1-1 was encoded in a pKK2.7 plasmid and was a generous gift from W. M. Atkins (University of Washington, Seattle) (*20*). This plasmid was previously modified so that the expressed protein contained a His_6 tag after the methionine at the N-terminus (*21*). In the current study, mutations were made to the plasmid containing the sequence for a His tag so that all mutant enzymes could be expressed as His-tagged proteins. The "QuikChange" kit from Stratagene was used for mutagenesis. The forward primers used for the mutants are as follows (codon that is used to mutate the amino acid is underlined): Y9F, 5′-CCA GTG CTT CAC TTC TTC AAT GCC CGG-3′; Y9T, 5′-CCA GTG CTT CAC ACC TTC AAT GCC CGG-3′; R15Q, 5′-GCC CGG GGC CAA ATG GAG TGC ATC CGG-3′; R131Q, 5′-GAC AGG ACC AAA AAC CAG TAC TTG CCT GCC-3′; R131M, 5′-GAC AGG ACC AAA AAC ATG TAC TTG CCT GCC-3′; R131E, 5′-GAC AGG ACC AAA AAC GAG TAC TTG-3′. Mutations were confirmed by the BigDye terminator cycle sequencing method performed on an ABI Prism model 377 DNA sequencer (PE Systems) at the Center for Agricultural Biotechnology, University of Delaware.

The wild-type enzyme was expressed without the His tag. All mutant enzymes were expressed with a His_6 tag at the N-terminus. However, it has previously been shown that the His tag does not affect the enzyme (*21*). Both wild-type and mutant enzymes were expressed in *Escherichia coli* strain JM105 as described by Vargo and Colman (*21*). In each case, 4 L of cell culture was grown at 37 °C and induced with 1 mM IPTG at 25 °C for 24 h. The cell culture was then centrifuged to obtain a pellet, which was resuspended in 10 mM Tris chloride buffer, pH 7.8 and then sonicated. The resulting supernatant was used to purify the enzyme.

Purification of Wild-Type GST and Mutant Enzymes. The supernatant was applied to an S-hexylglutathione column (for enzymes without a His tag) or a Ni-NTA column (for enzymes with a His tag), as described below. Purification using either column was conducted at 4 °C.

Wild-type GSTA1-1 without the His tag was purified by affinity chromatography using S-hexylglutathione Sepharose (*17*). In this method, the supernatant from 4 L of culture was applied to the column equilibrated with 10 mM Tris chloride buffer, pH 7.8. It was then washed with the same buffer, followed by elution of loosely bound proteins using 10 mM Tris chloride buffer, containing 0.2 M NaCl, pH 7.8. Finally, GSTA1-1 was eluted using 2.5 mM S-hexylglutathione in 10 mM Tris chloride buffer, pH 7.8, containing 0.2 M NaCl, concentrated, and dialyzed against 0.1 M potassium phosphate buffer containing 1 mM EDTA, pH 6.5.

The His-tagged enzymes were purified using Ni-NTA (*21*). In this method, the supernatant from 4 L of *E. coli* culture was applied to a Ni-NTA column (8 mL) equilibrated in 10 mM Tris chloride buffer, pH 7.8. It was washed with 10 mM Tris chloride, pH 7.8 containing 0.2 M NaCl to remove non-GST proteins. The enzyme was then eluted in 3 mL fractions, using a gradient of imidazole from 0 to 0.5 M in 10 mM Tris chloride, containing 0.2 M NaCl, pH 7.8 (100 mL of each buffer). The purity of fractions was determined by SDS−PAGE (12% polyacrylamide and 0.1% sodium dodecyl sulfate) using the method of Laemmli (*22*). Only those fractions containing pure enzyme were pooled, concentrated, and dialyzed against 0.1 M potassium phosphate buffer containing 1 mM EDTA, pH 6.5. All purified enzymes were stored in aliquots at −80 °C.

The concentration of purified enzymes was determined using $\epsilon_{270nm} = 22\,000\ M^{-1}\ cm^{-1}$ (*23*), and a molecular weight for each subunit of 25 500 Da. The purity of the protein was determined by SDS−PAGE (12% acrylamide, 0.1% sodium dodecyl sulfate). Finally, enzyme purity was confirmed by

[2] Formerly called GST4-4.

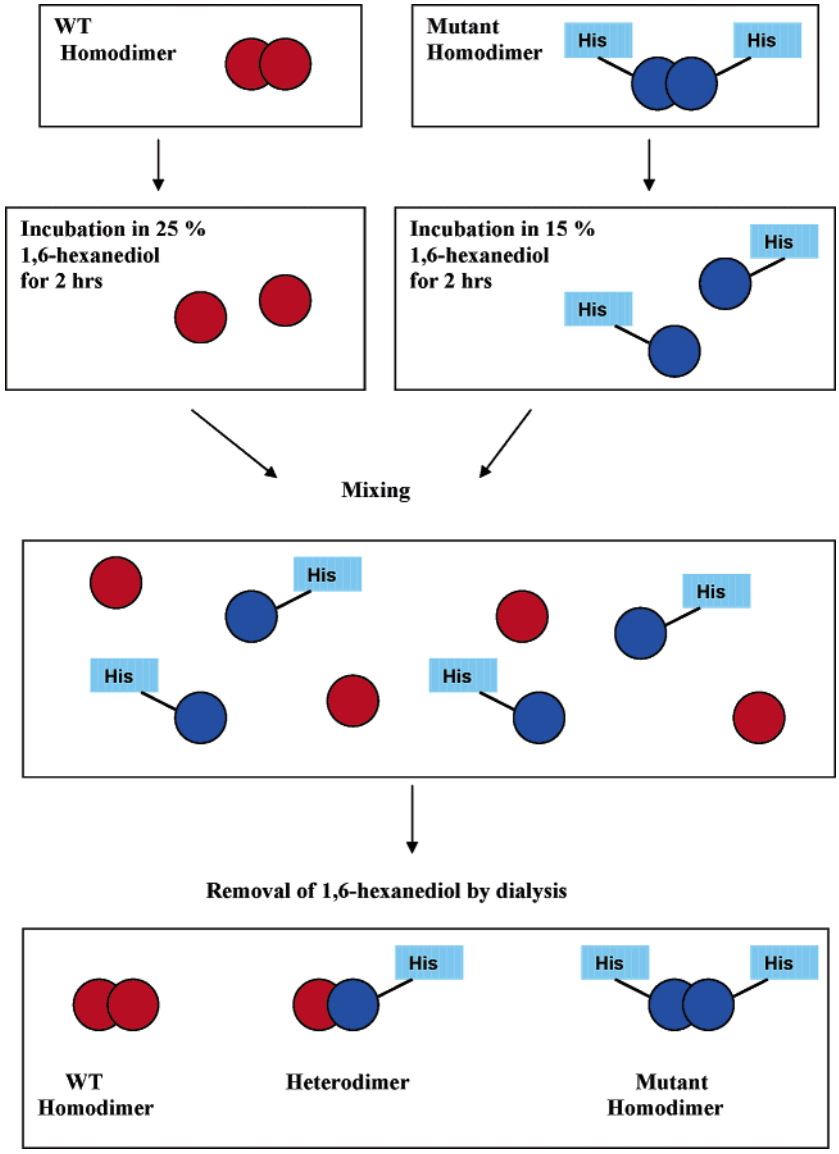

FIGURE 2: Schematic diagram showing generation of heterodimers. WT homodimer (1 mg) and 1 mg of mutant homodimer (with a His tag) were incubated separately in 25% and 15% 1,6-hexanediol, respectively, for 2 h, at 25 °C in 0.1 M potassium phosphate buffer, pH 7.5, containing 1 mM EDTA. The WT homodimer solution was diluted to 15% 1,6-hexanediol before mixing with mutant homodimer. The mixture was dialyzed overnight against 10 mM Tris chloride buffer, pH 7.8 containing 0.2 M NaCl, to generate the heterodimer.

gas-phase N-terminal sequencing using an Applied Biosystems Procise peptide sequence analyzer.

Standard Spectrophotometric Assay for GST Activity. The activity was determined by measuring the rate of increase in absorbance of the GSH−CDNB conjugate at 340 nm ($\Delta\epsilon = 9.6\ mM^{-1}\ cm^{-1}$) formed at 25 °C when 1 mM CDNB and 2.5 mM GSH are reacted with the enzyme in 0.1 M potassium phosphate buffer, pH 6.5 containing 1 mM EDTA (*24*). The enzyme activity was corrected for the nonenzymatic reaction between GSH and CDNB.

Generation of Heterodimers. Heterodimers were generated in which one subunit was wild-type (and without a His tag) and the other subunit had a single mutation (and a His tag). We have previously used acetonitrile in place of 1,6-hexanediol to form heterodimers. However, for some of the mutant enzymes, there was loss in activity in the presence of acetonitrile resulting in a lower yield of heterodimer. The yield improved when 1,6-hexanediol was used. The general scheme for formation of heterodimers is given in Figure 2. To dissociate the enzymes into subunits, wild-type enzyme (without a His tag) and mutant enzyme (with a His tag) were incubated separately in 25% and 15% (or 20%), respectively, in 1,6-hexanediol in 0.1 M potassium phosphate buffer, pH 7.5, containing 1 mM EDTA, for 2 h at 25 °C in a water bath. One milligram of each enzyme in 1 mL of buffer was used. The WT homodimer solution was diluted with buffer to give 15% of 1,6-hexanediol, and then mixed immediately with the mutant homodimer solution. This mixture was then dialyzed overnight against 10 mM Tris chloride buffer containing 0.2 M NaCl, pH 7.8 at 4 °C to remove 1,6-hexanediol and allow the re-formation of dimers (Figure 2). The mixture of two homodimers and one heterodimer was then loaded onto a Ni-NTA column (1.5 mL) equilibrated in 10 mM Tris chloride buffer, pH 7.8 containing 0.2 M NaCl, at 4 °C. The column was washed with the same buffer to remove unbound wild-type homodimer. The heterodimer and mutant homodimer were separated using a linear gradient from 10 mM Tris chloride, pH 7.8, containing 0.2 M NaCl to the same buffer containing 0.1 M imidazole (100 mL of each buffer). Fractions of 1 mL were collected and the

catalytic activity was determined under standard conditions. The three peaks were each pooled separately and concentrated to approximately 1 mL using the Amicon Ultra-15 centrifugal filter device (molecular weight cutoff = 10 kDa). In order to remove the imidazole and exchange the buffer, 9 mL of 0.1 M potassium phosphate buffer containing 1 mM EDTA, pH 6.5 was added to 1 mL of the concentrated protein sample, and the mixture was concentrated again to 1 mL in the Amicon Ultra-15 device. This procedure was repeated 3−4 times until the final concentration of imidazole was below 0.001 M. The activity of the recovered WT and mutant homodimers as well as the purified heterodimer was determined under standard conditions. The Bio-Rad protein assay, based on the Bradford method, was used to determine protein concentration, using wild-type His-tagged enzyme as a standard (*25*). All three enzymes were stored at −80 °C in 0.1 M potassium phosphate buffer, pH 6.5, containing 0.1 mM EDTA. The N-terminal sequences of the recovered homodimers and purified heterodimers were determined to confirm the purity of the enzymes.

Determination of Kinetic Parameters. The K_m^{GSH} was determined at a constant CDNB concentration of 2.5 mM, and the K_m^{CDNB} was determined at a constant GSH concentration of 2.5 mM or 10−12 mM, as indicated in Results. The CDNB was dissolved in ethanol, and 2.5% ethanol was maintained constant in all assays. The higher concentration of GSH was used for R131 mutant enzymes that exhibited high K_m values for GSH. The data were fit to a Michaelis−Menten plot of v versus [S], and the K_m and V_{max} were determined using "Sigma Plot".

Circular Dichroism Spectra. The CD spectra of enzyme samples were measured at room temperature in a cylindrical quartz cuvette of 0.1 cm path length using a Jasco model J-710 spectropolarimeter (Jasco, Inc., Easton, MD). Protein samples were in 0.1 M potassium phosphate buffer, pH 6.5, containing 1 mM EDTA. Concentrations of wild-type and mutant homodimers were 0.15 mg/mL. For heterodimers, the concentration ranged from 0.1 to 0.15 mg/mL. CD spectra were obtained in the wavelength range 200−250 nm. The resulting spectrum for each enzyme represents the average of five scans and has been corrected for any background due to buffer.

The CD spectrum for wild-type enzyme was compared in the absence and presence of 1,6-hexanediol. Wild-type enzyme in 0.1 M potassium phosphate buffer, pH 6.5, containing 1 mM EDTA was diluted with 1,6-hexanediol to give a final concentration of 25 vol %. The protein concentration was 0.15 mg/mL. As a control, the CD spectrum was determined using the same protein concentration and buffer conditions, except that 1,6-hexanediol was excluded from the solution.

Molecular Modeling. Insight II molecular modeling software (Molecular Simulations, Inc.) was used on an Indigo 2 work station (Silicon Graphics). The homology model of rat GSTA1-1 was constructed on the basis of the known crystal structure of human GSTA1-1. The rat GSTA1-1 and human GSTA1-1 share 76% identity plus 11% similarity in amino acid sequence, so the two are comparable in structure. Two crystal structures were considered, PDB 1GUH, the crystal structure complexed with the ligand, S-benzylglutathione, and PDB 1GSD, the crystal structure of the apo-enzyme (*14*, *26*). The ligand from 1GUH was overlaid with the structure of 1GSD, and this was subjected to energy minimization using the Discover program from Biosym. Steepest descent and conjugate gradient methods were used to reduce residual van der Waals overlaps. For modeling of the heterodimers, a single residue of one subunit was replaced by another residue and this was also subjected to energy minimization as described above.

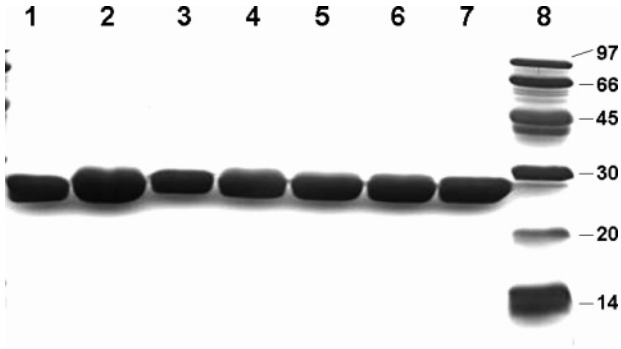

FIGURE 3: SDS−PAGE for purified wild-type and mutant enzymes of GSTA1-1. Purified protein (7 μg of each sample) was loaded in each lane. Lane 1: WT. Lane 2: Y9F. Lane 3: Y9T. Lane 4: R15Q. Lane 5: R131M. Lane 6: R131Q. Lane 7: R131E. Lane 8: Protein standards (with molecular weights given in kDa). Molecular weights of purified GSTs were about 25 kDa.

RESULTS

Mutagenesis and Expression. Tyr9, Arg15, and Arg131 residues were chosen as targets of mutagenesis, since these are some of the amino acid residues identified as active site residues in the crystal structure of GSTA1-1 (*14*). Tyr9 was replaced by phenylalanine and threonine. Arg15 was changed to glutamine. Three mutants of Arg131 were constructed: R131M, R131Q, and R131E. All mutations were confirmed by DNA sequencing, which also demonstrated that no mutations were introduced at positions other than the desired target.

Purification of Enzymes. Wild-type GSTA1-1 was purified by affinity chromatography using an S-hexylglutathione agarose column. The mutant enzymes contained a His_6 tag and hence were purified on the nickel-nitrilotriacetic acid (Ni-NTA) column. For all enzymes, SDS−PAGE showed a single band at 25 kDa indicating that the enzymes were purified to homogeneity (Figure 3). The wild-type enzyme migrated slightly lower than the mutant enzymes because of the absence of a His_6 tag. N-terminal sequencing confirmed the identity and purity of all enzymes. For the wild-type GSTA1-1, 10 mg of protein was obtained per liter of culture grown, while for the mutant enzymes (His-tagged), the yield was 50−60 mg per liter of culture grown.

Specific Activity of Wild-Type and Mutant Enzymes under Standard Conditions. The specific activities of all enzymes were determined (under standard conditions) at 2.5 mM GSH and 1 mM CDNB at 25 °C and pH 6.5 and are shown in Table 1. That of the wild-type enzyme is comparable to earlier reported values (*21*). Of the mutant enzymes studied here, the most drastic decreases in activity were observed for the Y9F, Y9T, and R15Q mutant enzymes (Table 1). The specific activity of Y9F was less than 1% that of wild-type, similar to previously reported values (*15*). Y9T and R15Q mutant enzymes were 14- to 50-fold less active than

Table 1: Specific Activities of Wild-Type and Mutant Enzymes under Standard Conditions[a]

enzyme	specific activity (μmol min^{-1} mg^{-1})
WT	61.5 ± 3.4
Y9F	0.5 ± 0.05
Y9T	0.035 ± 0.002
R15Q	0.01 ± 0.001
R131M	37.1 ± 2.5
R131Q	30.9 ± 1.4
R131E	14.8 ± 0.6

[a] Enzyme activity was measured spectrophotometrically from the rate of increase at A_{340nm}, the λ_{max} of the GSH−CDNB conjugate formed, using 2.5 mM GSH and 1 mM CDNB at 25 °C, in 0.1 M potassium phosphate buffer, pH 6.5 containing 1 mM EDTA. Specific activity is given with standard errors.

Y9F. In contrast, the R131 mutant enzymes exhibited specific activities closer to that of the WT enzyme: 60%, 50%, and 24% of that of the wild-type for R131M, R131Q, and R131E respectively,

CD Spectra of Mutant Enzymes. Wild-type enzyme and the mutant enzymes all exhibited minima at 220 and 210 nm, characteristic of a predominantly α-helical secondary structure. Representative spectra are shown in Figure 4. The CD spectra for all mutant enzymes were comparable to that of the wild-type enzyme, indicating that the mutations did not cause any marked change in secondary structure.

Generation of Heterodimers Using 1,6-Hexanediol. Heterodimers were generated in which one subunit was wild-type and the other was a mutant subunit with a single amino acid substitution in the active site. Heterodimers were generated with the following single mutations in the second subunit: Y9F, Y9T, R15Q, R131M, R131Q, and R131E. As outlined in Figure 2, 15−25% 1,6-hexanediol was used to dissociate the enzyme into monomers. Subsequent dialysis removed the 1,6-hexanediol and allowed random association to form dimers from a pool of two types of monomers. Three dimeric enzyme species were thus formed: WT homodimer, WT−mutant heterodimer, and mutant homodimer. Theoretically, the ratio among them should be 1:2:1, if association of the two types of monomers occurred randomly. Although this is the case when His-tagged WT is mixed with WT enzyme (*13*), when mutant and WT homodimers are mixed, the amount of heterodimer is lower; this observation probably reflects differences in affinity between the WT and the mutant monomer.

The two homodimers and newly formed heterodimer generated in each experiment were then separated using a Ni-NTA column, as described under Experimental Procedures. For each dimer mixture, separation on the Ni-NTA column yielded three peaks, as illustrated in Figure 5, for the separation of wild-type homodimer, WT−R131E heterodimer, and R131E homodimer. Since the wild-type homodimer lacks a His tag, it does not bind to the Ni-NTA column and was obtained as peak I, eluted in the starting buffer. The heterodimer contains one His tag (from the mutant subunit), and the mutant homodimer contains two His tags (one linked to each subunit). Since the affinity of protein for the Ni-NTA column depends on the number of His tags, these two proteins were separated using an imidazole gradient. The heterodimer eluted as peak II, while the mutant homodimer eluted as peak III. (Only the first half of the heterodimer peak was pooled in order to maximize purity of the heterodimeric species.)

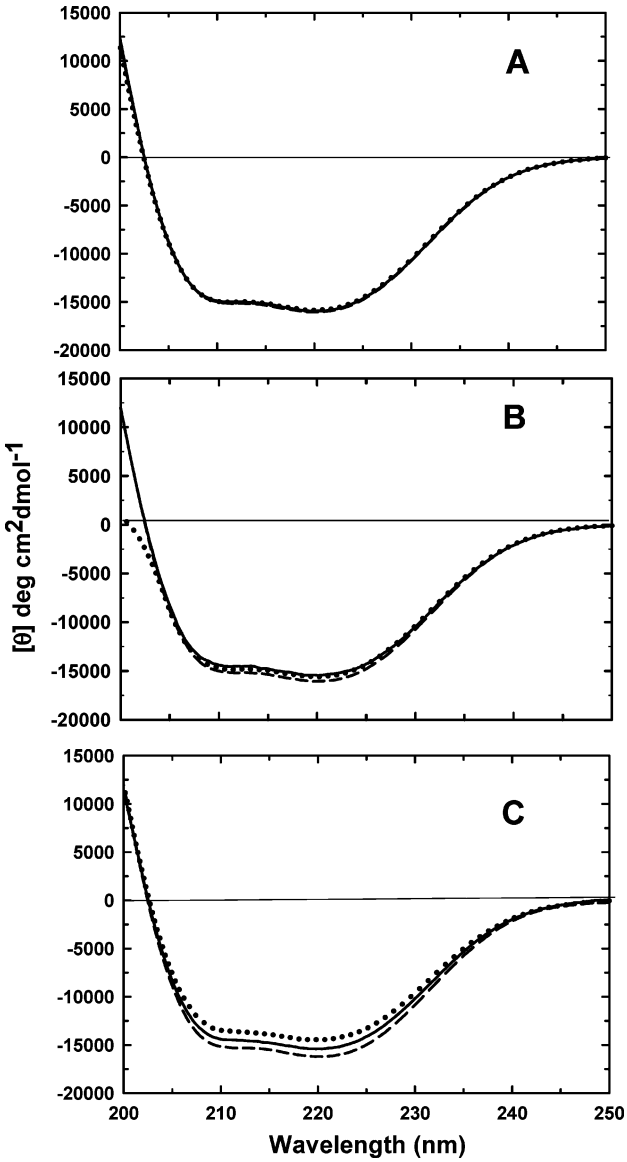

FIGURE 4: CD spectra of WT, mutant enzymes, and heterodimers. CD spectra of WT (dashed line), mutant (dotted line), and WT−mutant heterodimer (solid line) in 0.1 potassium phosphate buffer, pH 6.5, containing 1 mM EDTA. Protein concentrations used ranged from 0.1 to 0.15 mg/mL. (A) WT, R131M, and WT−R131M heterodimer. (B) WT, R131Q, and WT−R131Q heterodimer. (C) WT, R131E, and WT−R131E heterodimer.

The purity of all three enzymes recovered from the Ni-NTA column was determined by N-terminal sequencing as illustrated in Table 2 for the WT−R15Q heterodimer. These results are representative of those obtained for all heterodimers. The wild-type homodimer exhibited a single sequence of SGKPVLHYFNARGR at the N-terminus, while the mutant homodimer, containing a His tag, showed a single sequence of MHHHHHHSGKPVLH at the N-terminus. The heterodimer exhibited two PTH-amino acids at each cycle indicative of two sequences (one lacking the His tag and one with a His tag) present in a ratio of approximately 1:1. These results confirm the presence and purity of the heterodimer.

Stability of Heterodimers. It was important to ascertain whether the heterodimer was stable under the conditions of

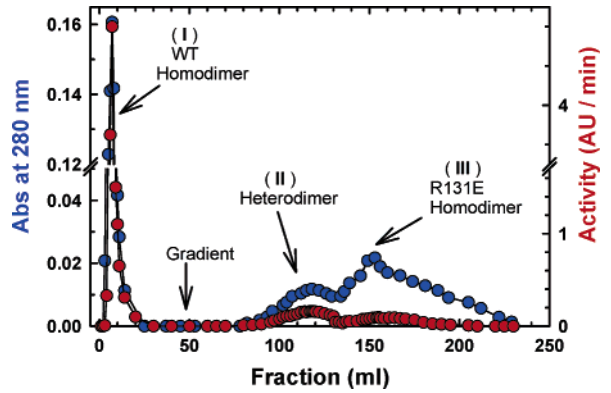

FIGURE 5: Separation of WT and R131E homodimers and WT−R131E heterodimer using a Ni-NTA column. The protein mixture was loaded onto a Ni-NTA column equilibrated with 10 mM Tris chloride buffer, pH 7.8, containing 0.2 M NaCl. The column was first washed with the same buffer to remove unbound WT homodimer. The heterodimer and R131E homodimer were separated using a gradient of 0−0.1 M imidazole in 10 mM Tris chloride buffer, pH 7.8, containing 0.2 M NaCl (100 mL of each buffer). Fractions were 1 mL each. Protein absorbance (blue circles) was measured at 280 nm. Activity (red circles) present in 30 μL of fraction was measured under standard conditions.

Table 2: N-Terminal Sequencing of WT−R15Q Heterodimer[a]

cycle	residue (non-His tag)	pmol	residue (His tag)	pmol
1	Ser	67	Met	111
2	Gly	56	His	36
3	Lys	98	His	58
4	Pro	64	His	55
5	Val	60	His	67
6	Leu	63	His	59
7	His	44	His	44
8	Tyr	62	Ser	54
9	Phe	59	Gly	51
10	Asn	48	Lys	70
11	Ala	67	Pro	47
12	Arg	45	Val	48
13	Gly	30	Leu	64
14	Ala	50	His	20
	average	51.6	average	50.6
	molar ratio: 1.02			

[a] An aliquot of purified heterodimer was subjected to N-terminal sequencing. Cycles 8−14 were considered for calculation of the molar ratio because the yield of PTH−His (cycles 2−7) is low and exhibits carryover in subsequent cycles, and hence gives inaccurate estimates of yields in these cycles.

purification and storage. To evaluate this issue, a sample of heterodimer from peak II (Figure 5) which had been stored at −80 °C in 0.1 M potassium phosphate buffer, pH 6.5, containing 1 mM EDTA was thawed and then reapplied to the Ni-NTA column under the same conditions as in Figure 5. Any dissociation of the heterodimer into its monomeric subunits would have resulted in new peaks, peak I and peak III, corresponding to the wild-type and mutant homodimers, respectively. However, the only peak of activity obtained was peak II, corresponding to the heterodimer. No GST activity was obtained in the wash fractions or in the second part of the gradient corresponding to the mutant homodimer. This result indicates that the heterodimer is stable in both the Tris chloride and phosphate buffers used for purification and storage, respectively. Furthermore, the specific activities did not change upon storage over a period of at least four months.

Table 3: Kinetic Parameters of WT, Y9F, Y9T, R15Q, and Heterodimers of Y9F, Y9T, and R15Q[a]

Enzyme	K_m^{GSH} (mM)	K_m^{CDNB} (mM)	V_{max} (μmol min^{-1} mg^{-1}) exptl	V_{max} (μmol min^{-1} mg^{-1}) theor:[b] heterodimers
WT	0.28 ± 0.04	0.79 ± 0.2	68.7 ± 5.7	
Y9F	1.2 ± 0.12	0.63 ± 0.05	1.3 ± 0.05	
WT−Y9F	0.14 ± 0.01	0.65 ± 0.06	**22.2** ± 1.2	34.8
Y9T	[c]	[c]	0.13[d] ± 0.012	
WT−Y9T	0.14 ± 0.01	0.72 ± 0.09	**19.1** ± 0.3	34.4
R15Q	[c]	[c]	0.018[d] ± 0.005	
WT−R15Q	0.15 ± 0.01	0.62 ± 0.06	**27.1** ± 0.5	34.3

[a] All assays were performed at 25 °C in 0.1 M potassium phosphate buffer, pH 6.5, containing 1 mM EDTA. The K_m^{GSH} was determined by maintaining the concentration of CDNB constant at 2.5 mM with GSH concentrations varying from 0.05 to 10 mM, while K_m^{CDNB} was determined at a constant GSH concentration of 2.5 mM and varying concentrations of CDNB from 0.02 to 4 mM. All values are reported with standard errors. [b] The theoretical values of V_{max} represent the expected V_{max} of the heterodimer if the activity of each subunit is not influenced by that of the other. It was calculated as follows: Theoretical V_{max} = ($^1/_2V_{max}$ of wild-type homodimer + $^1/_2V_{max}$ of mutant homodimer). [c] Extremely low activities for Y9T and R15Q, together with significant background rates at high GSH and CDNB concentrations, did not allow the determination of K_m for these mutant enzymes. [d] These values were determined at 10 mM GSH and 4 mM CDNB.

Activity of Recovered Enzymes. The proteins recovered from the Ni-NTA column were evaluated for activity. The specific activities of the wild-type and mutant homodimers under standard conditions were the same as the initial specific activities of these enzymes before mixing in 1,6-hexanediol. In a control experiment, a WT−WT^{His} dimer was generated with one subunit lacking a His tag and the other subunit having a His tag. The activity of this isolated WT−WT^{His} dimer was the same as that of the WT−WT or WT^{His}−WT^{His} homodimers. In contrast, the specific activities of all WT−mutant heterodimers were found to be *lower* than the average of the specific activities of the two corresponding homodimers. An average value would be expected if the activity of each subunit was independent of the other. This suggests that the two active sites must interact with each other.

Kinetic Parameters of Wild-Type and Mutant Enzymes. The K_m^{GSH}, K_m^{CDNB}, and V_{max} for wild-type and mutant enzymes are given in Tables 3 and 4. Kinetic parameters for the wild-type enzyme are comparable to previously reported values (*21*). Y9F exhibited a V_{max} of 1.3 μmol min^{-1} mg^{-1}, less than 2% of that of the WT enzyme (Table 3), comparable to the V_{max} reported earlier (*15, 16*). Y9F has a K_m^{GSH} which is four times that of wild-type enzyme. Y9T and R15Q mutant enzymes exhibited extremely low activities, precluding the determination of K_m values for these mutants. These results indicate that Tyr9 and Arg15 have catalytic roles and are critical for the activity of the enzyme.

Each active site has Arg131 contributed from the opposite subunit; i.e., Arg131 belongs to subunit B but is part of the active site of subunit A (Figure 1). To evaluate the importance of a positive charge at this position, this residue was replaced by methionine, glutamine, and glutamate, with the results shown in Table 4. The V_{max} values of R131M and R131Q are not appreciably different from that of the WT enzyme. However, R131E exhibits a V_{max} that is 50% that of the wild-type. The K_m^{CDNB} for all mutant enzymes is comparable to that for the wild-type enzyme, indicating that

Table 4: Kinetic Parameters of WT, R131 Mutant Homodimers, and Heterodimers of These Mutant Enzymes[a]

enzyme	K_m^{GSH} (mM)	K_m^{CDNB} (mM)	V_{max} (μmol min^{-1} mg^{-1}) exptl	V_{max} (μmol min^{-1} mg^{-1}) theor:[b] heterodimers
WT	0.28 (± 0.04)	0.79 (± 0.2)	68.7 (± 5.7)	
R131M	1.0 (± 0.01)	0.64 (± 0.1)	64.3 (± 3.9)	
WT−R131M	0.25 (± 0.1)	0.51 (± 0.1)	**39.7** (± 5.9)	66.5
R131Q	0.82 (± 0.1)	0.64 (± 0.1)	54.2 (± 5.0)	
WT−R131Q	0.38 (± 0.05)	0.9 (± 0.2)	**48.5** (± 4.0)	61.5
R131E	2.1 (± 0.3)	0.8 (± 0.1)[c]	34.8 (± 1.1)	
WT−R131E	0.24 (± 0.03)	0.42 (± 0.2)	**24.9** (± 2.9)	51.7

[a] Assays were conducted at 25 °C in 0.1 M potassium phosphate buffer, pH 6.5, containing 1 mM EDTA. All values are reported with standard errors. The K_m^{GSH} was determined with GSH concentrations varying from 0.05 to 10 mM and a constant [CDNB] = 2.5 mM. For the determination of K_m^{CDNB}, the CDNB concentration was varied from 0.02 to 4 mM, while the concentration of GSH was kept constant at 10 mM. [b] The theoretical values of V_{max} represent the expected V_{max} of the heterodimer if the mutation in one subunit had no effect on the V_{max} in the other subunit. It was calculated as follows: Theoretical V_{max} = ($^1/_2V_{max}$ of wild-type homodimer + $^1/_2V_{max}$ of mutant homodimer). [c] The K_m^{CDNB} and V_{max} were also determined at 25 mM GSH and found to be the same as that at 10 mM GSH.

affinity of the enzyme for CDNB is not affected by mutations at position 131. In contrast, the values of K_m^{GSH} for all three position 131 mutant enzymes are increased as compared to the wild-type: replacement of Arg131 by Met or Gln yields enzymes with K_m^{GSH} about three times that of wild-type, while substitution by the negatively charged residue, glutamate, results in an 8-fold increase in K_m^{GSH}. This effect on K_m^{GSH} indicates that Arg131 participates in glutathione binding.

Kinetic Parameters of Heterodimers. The heterodimers considered in this study contained one wild-type subunit and one subunit with a single mutation in the active site, allowing us to evaluate the effect of a mutation in one subunit on the activity of the other subunit. Tyr9 and Arg15 contribute to the active site of their own subunit. On the other hand, Arg131 contributes to the active site of the other subunit. For all heterodimers, the experimental maximum velocity was compared to a theoretical value (Tables 3 and 4). The theoretical value is the value expected if the activity of each subunit is independent of the other, and is calculated as the sum of maximum velocities of individual subunits. Figure 6 shows representative Michaelis−Menten plots for two heterodimers, WT−R131E and WT−R131M. The V_{max} for both heterodimers is much lower than the theoretical value. All heterodimers give a V_{max} lower than the theoretical value, ranging from 48% to 79% of the expected values (Tables 3 and 4). Since the specific activities of the heterodimers did not change over several months of storage, these results do not reflect a time-dependent instability of the heterodimers. Although the K_m^{GSH} values for the mutant homodimers of R131 mutants are between 0.8 and 2.1 mM, the K_m^{GSH} values of the corresponding heterodimers were between 0.24 and 0.38 mM, comparable to that for the WT enzyme (Table 4). The K_m^{CDNB} of these heterodimers was also not significantly different from that of the WT enzyme (Table 4), an indication that the affinity for CDNB is not affected in the heterodimers.

Circular Dichroism Spectra of Heterodimers. Since the activity of heterodimers was lower than the expected theoretical values, it was important to establish whether this

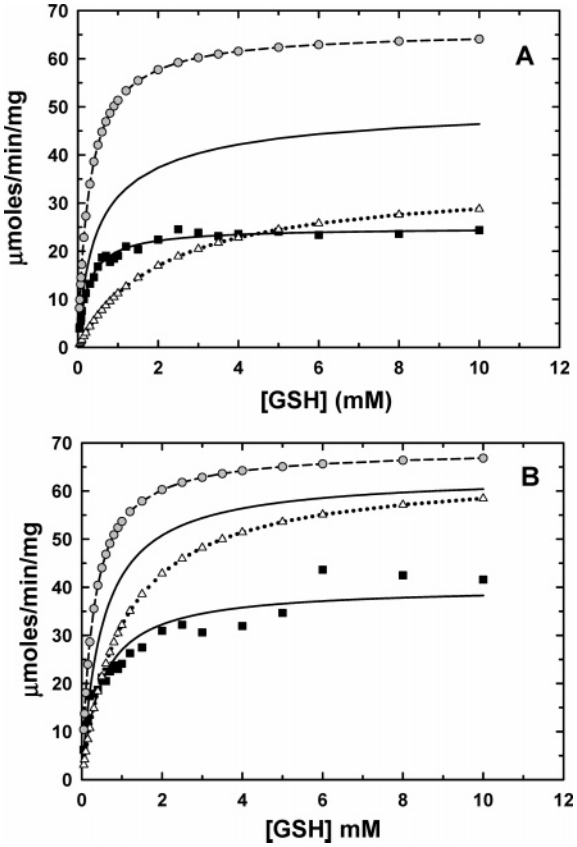

FIGURE 6: Michaelis−Menten plots for heterodimers WT−R131E and WT−R131M. Two representative plots are shown here. The velocities were determined at [CDNB] = 2.5 mM, in 0.1 M potassium phosphate buffer, pH 6.5, containing 1 mM EDTA, at 25 °C. A plot of velocity versus GSH concentration is given for WT−R131E heterodimer (A) and WT−R131M heterodimer (B). In each panel, plots for wild-type enzyme (circles with dashed line), mutant homodimer (triangles with dotted line), and heterodimer (squares with solid line) are shown. The experimental plot for the heterodimers is compared to a theoretical plot (solid line without symbol). The theoretical plot for the heterodimer is generated by determining the velocity at a given substrate concentration as follows: v = ($^1/_2v$ of wild-type homodimer + $^1/_2v$ of mutant homodimer).

loss in activity resulted from a change in secondary structure in the heterodimer. CD spectra were obtained for the heterodimers and compared to those of the WT and mutant homodimers. Figure 4 shows CD spectra of the three heterodimers with a mutation at position 131. There was no appreciable change in the spectra, indicating that formation of heterodimers does not cause any alteration in the secondary structure of the enzyme. Furthermore, the CD spectra did not change over a period of at least four months of storage, indicating that the heterodimers are structurally stable.

Effect of 1,6-Hexanediol on Enzyme Structure. The mechanism by which 1,6-hexanediol dissociates GST dimers and promotes heterodimer formation is not known. It is not evident whether 1,6-hexanediol caused dimers to dissociate as a result of unfolding or if the solvent stabilizes GST monomers allowing the dimers to dissociate easily. To evaluate the effect of 1,6-hexanediol on the enzyme, CD spectra of wild-type GSTA1-1 were compared in the absence and presence of 1,6-hexanediol (Figure 7). The CD spectra are distinguishable in buffer alone and in buffer containing 1,6-hexanediol. Both exhibit similar minima around 208 and

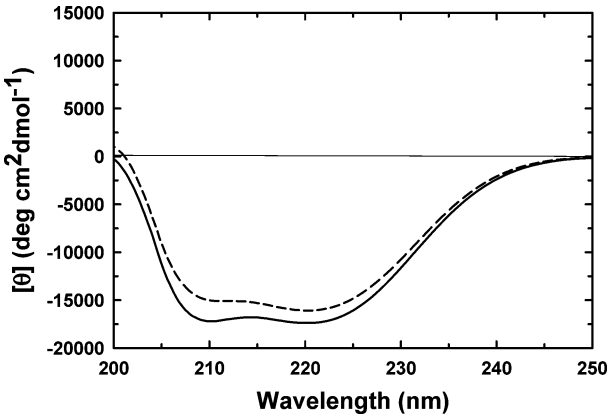

FIGURE 7: Comparison of CD spectra in buffer and 1,6-hexanediol. The CD spectra for wild-type in buffer (dashed line) and 25% 1,6-hexanediol (solid line) were determined using a protein concentration of 0.15 mg/mL in 0.1 M potassium phosphate buffer, pH 6.5, containing 1 mM EDTA, at room temperature.

220 nm; however, in 1,6-hexanediol, the magnitude of the minimum at 208 nm is greater. Estimation of the α-helical structure (*27*) gave values of 60% and 65% for CD spectra in the absence and presence of 1,6-hexanediol, respectively. The slight increase in helical structure suggests that 1,6-hexanediol stabilizes the secondary structure in the monomer subunits.

DISCUSSION

The alpha class glutathione S-transferase exists in solution predominantly in dimeric form. Whether the two active sites of the dimer function independently or communicate with each other is an important unresolved issue. Ricci et al. (*28*) had earlier pointed out that the two subunits of horse erythrocyte GST are nonequivalent in their reaction with sulfhydryl reagents, although others have said that the subunits function independently.

Heterodimers, containing one wild-type subunit and a subunit with a mutation in the active site, offer a means of studying subunit interactions. In the current study, three amino acid residues were mutated: Tyr9, Arg15, and Arg131. The role of Tyr9 and Arg15, residues that contribute to the activity in the same subunit, had already been established (*15*, *16*, *19*). Our study establishes the effect of these two residues on the activity of the opposite subunit, and hence in the dimer as a whole. In contrast, Arg131 has never been studied before. We investigated its role in the active site to which it directly contributes, as well as its effect on the activity of the second subunit.

Tyr9 is conserved among the cystolic GSTs and was the first amino acid identified as important for catalysis (*15*). Our study indicates that V_{max} values of Y9F and Y9T mutant enzymes are less than 2% of that of the wild-type. This is in accordance with earlier reported values (*15*, *16*). Tyr9 acts as a H-bond donor and stabilizes the thiolate of GSH prior to its attack on the electrophilic substrate. Replacement of Tyr by Phe eliminates this stabilizing effect, resulting in very low activity, and a 4-fold increase in K_m^{GSH} for this mutant enzyme. This result is in agreement with those obtained by Stenberg et al. (*15*). In the Y9T mutant enzyme, the hydroxyl group of Thr has the potential for H-bonding; nevertheless its specific activity is still very low as compared to the WT enzyme. This is because its hydroxyl group is positioned further away from the sulfur of GSH (5 Å), eliminating the possibility of H-bonding with the thiol group of GSH. The specific activity of the Y9T mutant enzyme is 10-fold lower than that of the Y9F mutant enzyme, indicating the importance of the aromatic ring. The aromatic ring of Tyr9 is situated 3 Å away from that of Phe10. This distance is sufficiently close for a $\pi-\pi$ stacking interaction (less than 5.6 Å) (*29*). In addition, the aromatic ring of Tyr9 and that of the benzyl group (of S-benzylglutathione) in the crystal structure are 5.2 Å apart. The position of the benzyl group represents that of the electrophilic substrate (in this case, CDNB) in the enzyme. Replacement of Tyr by Thr at position 9 would therefore interfere with the interaction between these aromatic rings around the active site leading to local disturbance around the active site.

The role of Arg15 is unique to the alpha class GSTs (*2*). The importance of a positive charge at position 15 has already been established (*19*). The N^{ϵ} of Arg15 and the cysteinyl sulfur of GSH are 3.8 Å apart and are involved in an electrostatic interaction. The peptidyl nitrogen of Arg15 also H-bonds to the hydroxyl group of Tyr9 (distance between the two groups is 3 Å). Thus, together with Tyr9, Arg15 stabilizes the thiolate ion. In a previous study, mutation of Arg15 to Leu, Lys, and His resulted in mutant enzymes that were less active than the wild-type, with the lowest activity exhibited by the R15H mutant enzyme (*19*). In our study we mutated Arg15 to Gln, resulting in a 40-fold lower activity than that of the R15H mutant of the previous study. Thus, although the side chain of Gln has the ability to form a H-bond, it apparently does not do so, perhaps because the shorter side chain of Gln is not positioned to interact with the −SH of GSH or the −OH of Tyr9.

The exact role of Arg131 has not been established, although the crystal structure of human GSTA1-1 shows that Arg131 is 2.5 Å away from the glycine carboxylate of GSH bound in the opposite subunit (Figure 1) (*14*). We generated three mutants, (R131Q, R131M, and R131E) to test the effect of substituting the positively charged side chain of Arg with the neutral Met (which lacks H-bonding potential), neutral Gln (which has the ability to form H-bonds) and with the negatively charged Glu. Met, Gln and Glu are all similar in size. As compared to the K_m^{GSH} for WT, the K_m^{GSH} is approximately 3-fold higher for the R131M and R131Q mutant enzymes, and 10-fold higher for the R131E mutant enzyme. In the WT enzyme, the positive charge of arginine is neutralized by the negative charge of the carboxylate of GSH. In R131M and R131Q, this electrostatic attraction is lost, while in R131E, the favorable interaction is replaced by a repulsive interaction between the negatively charged carboxylate of Glu131 and the negative carboxylate (C-terminus end) of GSH. As a result, binding of GSH in the R131E mutant enzyme is weaker than in the R131M and R131Q mutant enzymes. A distortion in GSH binding can also account for the low activity for the R131E mutant enzyme. The K_m^{CDNB} of all mutant enzymes were comparable to that of the WT, indicating that the CDNB binding site was not appreciably altered as a result of these mutations.

The Y9, R15, and R131 mutant homodimers were used to form heterodimers, which were generated after incubation of WT and mutant enzyme in 1,6-hexanediol. In solution, GSTs exist in a monomer−dimer equilibrium with the dimer

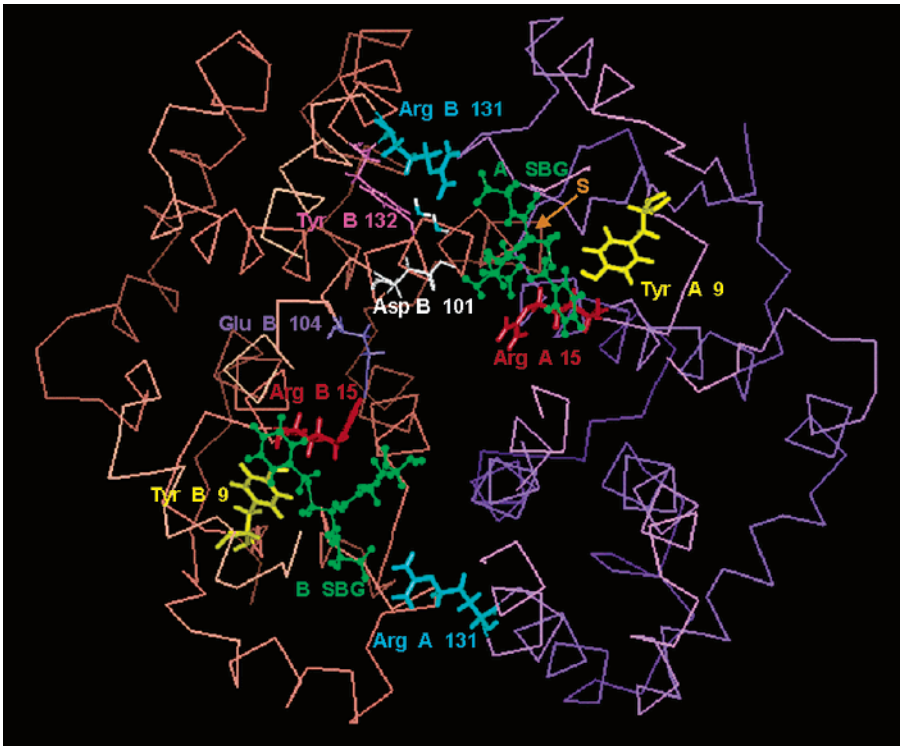

FIGURE 8: Structure of GSTA1-1 as viewed from the bottom of the cleft. Subunits A and B are shown in purple and orange, respectively. The inhibitor S-benzyl glutathione, SBG (green), is shown bound in both active sites. The residues (Tyr9, Arg15, and Arg131) mutated in the heterodimers are shown in thick lines, while the residues (Tyr 132, Asp 101, and Glu104) that are part of the connectivity between the two active sites are shown in thin lines. The water molecules are indicated by blue and white lines.

form predominating. Hydrophobic interactions exist at the dimer interface, and these are important for maintaining the structure of the dimer (*21*). 1,6-Hexanediol most likely binds to the hydrophobic regions at the interface, inhibiting dimerization of the subunits, and increasing the concentration of monomeric species. Le Trong et al. recently identified a network of water molecules connecting the two active sites (*30*); this network of water molecules may play a role in holding the subunits together. The hydroxyl groups of 1,6-hexanediol may compete with the water molecules for hydrogen bonding with the side chains of the protein's amino acids, resulting in the dimer−monomer equilibrium shifting toward monomer.

The CD spectrum of GSTA1-1 in 25% 1,6-hexanediol indicates that there is no decrease in the percentage of helical structure, suggesting that monomers are formed without unfolding of each subunit. Alcohols have previously been shown to preserve the secondary structure of proteins while altering the tertiary structure (*31*). In contrast to the observations for urea solutions (*32*), it appears, therefore, that the monomeric form of alpha GST in 1,6-hexanediol is quite stable structurally. Although a stable monomer can be obtained, the dimer form is required for maximum activity (*21*).

The study of subunit interactions is important for many enzymes. Typically guanidinium chloride or urea is used to dissociate dimers and form heterodimers. We initially used acetonitrile to dissociate the dimer, but found that many mutant enzymes were unstable in this solvent and precipitated easily. All of these reagents cause unfolding of the enzyme and, in some cases, loss of activity. As an alternative, 1,6-hexanediol may offer a better means of promoting heterodimer formation not only for GSTs but for other enzymes as well.

The heterodimers, with one mutant enzyme and one wild-type subunit, allowed evaluation of the effect of one subunit on the opposite subunit. In all of the heterodimers we tested, the activity of the wild-type subunit was affected when either Tyr9, Arg15, or Arg131 was mutated in the other subunit. In GSTA1-1, several residues are in contact with the substrate, of which Arg131 and Asp101 are contributed from the opposite subunit. These two residues may play a role in communication between the two active sites. On the basis of the crystal structure of GSTA1-1 (*14*), Arg131 and Asp101 of the same subunit do not communicate directly with each other (the minimum distance between them is 7 Å); however, they do communicate via the glutathione of the other subunit. As shown in Figure 8, the guanidino group of R131 (B) and the C-terminus carboxylate of GSH (A) are involved in an electrostatic interaction. The N-terminal amino group of GSH (A) interacts with Asp101 (B) via a salt link. The peptide oxygen of Asp101 (B) is within H-bonding distance (3.2 Å) of the peptide nitrogen of Glu104 (B) situated three residues away on the same helix. The carboxylate of Glu104 (B) is involved in an electrostatic interaction with the amino group of Arg15 (B). Arg15 (B) in turn interacts directly with the GSH (B). This connectivity has also been pointed out by Le Trong et al. (*30*). In addition, they have located a water molecule interacting with Asp101 and Tyr132 in the same subunit. This water molecule is 2.7 Å away from the carboxylate of Asp101 and 2.6 Å from the hydroxyl of Tyr132, which is adjacent to Arg131. We have also located a second water molecule (shown in Figure 8) connecting Tyr132 and Arg131, at a distance of 2.7 Å from the hydroxyl

of Tyr132 and 2.9 Å away from the guanidino group of Arg131. Hence Arg131 and Asp101 are connected not only via the GSH of the opposite subunit but also through Tyr132 and the two water molecules. Therefore mutation of Arg131 in subunit B will result in perturbation of the active site in subunit A, which will then be transferred through Asp101 and Glu104 to Arg15 in subunit B. Similarly any perturbation around the active site of subunit A as a result of mutation of Tyr9 (A) or Arg15 (A) will be communicated via Asp101 (B), to the active site of B, thus accounting for our observation that the V_{max} of all heterodimers was lower than expected. Also, the network of water molecules may play a role in communication between the two active sites. Most of these solvent molecules connect to side chains of the protein. Therefore, a perturbation occurring in one active site may very well be communicated to the other active site through this intricate network of water molecules. The lowered maximum velocities in our heterodimers support this theory.

Mutation of Tyr9 to either Phe or Thr in one subunit affected catalysis in the wild-type subunit. WT−Y9F and WT−Y9T both exhibited V_{max} values 56−63% of the expected values. Any perturbation of the substrate in subunit A caused as a result of mutation of Tyr9 would be transferred to the active site of subunit B, via Asp101(B) as described earlier.

The alpha class of GSTs is characterized by a C-terminal helix which covers the active site when the GSH conjugate is bound to the enzyme (*30*, *33*). The C-terminus thus plays a role in the binding and release of substrate and product, respectively (*34*, *35*, *36*). In the alpha class of GSTs, the rate-limiting step is product release, and the conformation of the C-terminus is hence important for catalysis. Phe220, a residue of the C-terminus helix, has its aromatic ring 4.3 Å from that of Phe10. Phe222, situated at the end of the C-terminal helix, is 5.2 Å from the benzyl ring of the reaction product, which in turn is 4.7 Å from the aromatic ring of Phe10. Therefore Phe10 interacts directly and indirectly with Phe220 and Phe222, respectively. Le Trong et al. postulated that the orientations of Phe10 and Phe222 are interdependent and play a role in determining the conformation of the C-terminus during ligand binding (*30*), while Nilsson et al. showed that Phe220 and Phe222 influence catalysis in GSTA1-1 (*34*). It has been shown that the ionization of Tyr9 and the dynamics of the C-terminal are associated (*35*, *36*). Mutation of Tyr9 to Thr will interfere with the $\pi-\pi$ interaction that exists between Tyr9 and Phe10. Construction of an energy minimized model of the Y9T mutant enzyme shows that the aromatic ring of Phe10 is oriented slightly differently in the mutant enzyme as compared to the WT enzyme. Moreover, the mutation increases the distance between Phe10 and Phe222 (from 5.7 Å to 7.5 Å), as well as the distance between Phe10 and the S-benzyl ring of substrate. By affecting the orientations of Phe10, Phe220, and Phe222, the replacement of Tyr9 by Thr may alter the dynamics of the C-terminal region, and hence the rate-limiting step in the reaction. Structural perturbations around this region are likely to be transmitted to the other active site as well. Similar perturbations may account for the previous report that modification of Met208 of one subunit of GSTA1-1 by the photoaffinity label glutathionyl S-[4-succinimidyl]benzophenone causes inactivation of both subunits (*10*). Met208 is located at the start of the C-terminal helix, and the effect of its modification may be communicated to the active site of the same subunit by the change in the Phe220, Phe222, and Phe10 interaction, while the effect is transmitted to the second subunit through interaction of the reagent's glutathionyl moiety with Asp101 and Arg131 of the second subunit.

Mutation of Arg15 to Gln removes the electrostatic interaction between Arg15 and Glu 104. In the crystal structure, the distance between the amino group of Arg15 and carboxyl of Glu104 in the WT enzyme is 2.9 Å. In contrast, in the energy-minimized model of the R15Q mutant enzyme, the distance between the amino acids at position 15 and 104 increases to 5.8 Å, due to the loss of electrostatic attraction between the two groups. The methylene groups of Arg15 are also involved in the binding of the hydrophobic substrate. Replacement of Arg by Gln shortens the side chain length, which may cause adjustments of the position of Gln in order to interact with the sulfur of GSH and the tyrosyl hydroxyl group. Thus, mutation of Arg15 to Gln decreases the communication to the opposite subunit. This may explain why the effect on the other subunit is the least in the WT−R15Q heterodimer, among all the heterodimers studied here.

In the heterodimers in which Arg131 of one subunit is mutated, the V_{max} values of all three heterodimers were lower than the expected values. The most drastic effect was seen in the WT−R131E heterodimer, which exhibited a V_{max} that is 48% of the expected value for the heterodimer. Although R131 of subunit B is far away from active site B, it does communicate with it via the active site of subunit A. Modeling studies indicate that the guanidino group of Arg131 is 3.5 Å from the glycyl carboxyl of GSH, but when replaced by Glu, the carboxyl groups of Glu131 and GSH mutually repel one another, resulting in the increased distance of 7.4 Å between the two. Moreover, Glu131 becomes close (3.2 Å) to Lys127 for charge neutralization. Thus, replacement of a positive charge by a negative charge at 131 results in disruption of important interactions, and formation of new ones, leading to perturbation around the active site of one subunit, which can then be transmitted through Asp101 and Glu104, to Arg15 in subunit B.

Surprisingly, the K_m^{GSH} of the heterodimers are comparable to that of the WT homodimer. It appears that binding of GSH in the WT subunit of the heterodimer actually facilitates the binding of GSH in the other subunit. In the heterodimer, the presence of one Arg131 is apparently sufficient to position the subunits in a favorable orientation so that GSH binding is not affected even in the other mutated active site. However, if Arg131 is mutated in both subunits (as in the mutant homodimer), the positioning of GSH in both subunits is disrupted, resulting in a decreased affinity for GSH in both active sites, as indicated by the high K_m^{GSH} in the Arg131 mutant homodimers.

Our results with heterodimers of R131 mutant enzymes are in contrast with those obtained by Lien et al. for heterodimers of Asp101 mutant enzymes (*12*). In their study, replacement of Asp101 by Lys in one subunit had no effect on the CDNB conjugating activity of the other wild-type active site. In that case, the positive charge of Lys (in the WT−D101K heterodimer) would be repelled by the positively charged N-terminal of GSH, probably leading to an altered position of Lys101. According to the wild-type model

structure, the carboxylate of Asp101 is 3.1 Å away from the N-terminal amino group of GSH. We modeled the WT−D101K heterodimer by replacing Asp101 by Lys in one subunit. In this model, Lys moves away from GSH, placing the amino group of Lys 5.6 Å away from the amino group of GSH, and closer to Glu97 (3.5 Å). This movement results in the positive charge of Lys being stabilized by the negatively charged Glu97; the connectivity between Lys101 (B) and GSH (A) is thereby disrupted. This scenario may account for the failure of Lien et al. (*12*) to observe communication between the active sites in the reaction between GSH and CDNB.

In the present study, we have generated heterodimers containing a WT subunit and a subunit with a single mutation in the active site. The use of heterodimers in the investigation of subunit interaction has been undertaken previously (*12*, *13*); however, this is the first study investigating the activity of heterodimers, in which residues contributing to the active site in the same subunit were mutated. All the heterodimers we examined exhibited lower than expected activity, indicating that a mutation in one active site perturbs the structure in such a way that the other active site is also affected. Thus, any change in the local environment of the active site can cause a structural perturbation in parts of the enzyme that are situated far from that active site. This communication is of a complex nature and not only takes place through the side chains of various amino acids but also may involve the network of water molecules that connect the two active sites.

ACKNOWLEDGMENT

We wish to thank Dr. Melissa Vargo for her help and suggestions at the start of this project, and Dr. Yu Chu Huang for N-terminal sequencing of the proteins.

REFERENCES

1. Johansson, A. S., and Mannervik, B. (2001) Human glutathione transferase A3-3, a highly efficient catalyst of double-bond isomerization in the biosynthetic pathway of steroid hormones, *J. Biol. Chem. 276*, 33061−33065.
2. Armstrong, R. N. (1997) Structure, catalytic mechanism, and evolution of the glutathione transferases, *Chem. Res. Toxicol. 10* (1), 2−18.
3. Hayes, J. D., and Pulford, D. J. (1995) The glutathione S-transferase supergene family: regulation of GST and the contribution of the isoenzymes to cancer chemoprotection and drug resistance, *Crit. Rev. Biochem. Mol. Biol. 30* (6), 445−600.
4. Adler, V., Yin Z., Fuchs, S. Y., Benezra, M., Rosario, L., Tew, K. D., Pincus, M. R., Sardana, M., Henderson, C. J., Wolf, C. R., Davis, R. J., and Ronai, Z. (1999) Regulation of JNK signaling by GSTp, *EMBO J. 18*, 1321−1334.
5. Townsend, D. M., and Tew, K. D. (2003) The role of glutathione-S-transferase in anti-cancer drug resistance, *Oncogene 22*, 7369−7375.
6. van Ommen, B., Bogaards, J. J., Peters W. H., Blaauboer, B., van Bladeren, P. J. (1990) Quantification of human hepatic glutathione S-transferases, *Biochem. J. 269*, 609−613.
7. McHugh, T. E., Atkins, W. M., Racha, J. K., Kunze, K. L., and Eaton, D. L. (1996) Binding of the aflatoxin-glutathione conjugate to mouse glutathione S-transferase A3-3 is saturated at only one ligand per dimer, *J. Biol. Chem. 271*, 27470−27474.
8. Vargo, M. A., and Colman, R. F. (2000) Affinity labeling of rat glutathione S-transferase isozyme 1-1 by 17beta-iodoacetoxy-estradiol-3-sulfate, *J. Biol. Chem. 276*, 2031−2036.
9. Wang J., Bauman, S., and Colman, R. F. (1998) Photoaffinity labeling of rat liver glutathione S-transferase, 4-4, by glutathionyl S-[4-(succinimidyl)-benzophenone], *Biochemistry 37*, 15671−15679.
10. Wang J., Bauman, S., and Colman, R. F. (2000) Probing subunit interactions in alpha class rat liver glutathione S-transferase with the photoaffinity label glutathionyl S-[4-(succinimidyl)benzophenone], *J. Biol. Chem. 275*, 5493−5503.
11. Danielson, U. H., and Mannervik, B. (1985) Kinetic independence of the subunits of cytosolic glutathione transferase from the rat, *Biochem. J. 231*, 263−267.
12. Lien, S., Gustafsson, A., Andersson, A. K., and Mannervik, B. (2001) Glutathione transferase A1-1 demonstrates both half-of-the-sites and all-of-the-sites reactivity, *J. Biol. Chem. 276*, 35599−35605.
13. Vargo, M. A., Colman, R. F. (2004) Heterodimers of wild-type and subunit interface mutant enzymes of glutathione S-transferase A1-1: interactive or independent active sites? *Protein Sci. 13*, 1586−1593.
14. Sinning, I., Kleywegt, G. J., Cowan, S. W., Reinemer, P., Dirr, H. W., Huber, R., Gilliland, G. L., Armstrong, R. N., Ji, X., Board, P. G., Olin, B., Mannervik, B., and Jones, T. A. (1993) Structure determination and refinement of human alpha class glutathione transferase A1-1, and a comparison with the Mu and Pi class enzymes, *J. Mol. Biol. 232*, 192−212.
15. Stenberg, G., Board, P. G., and Mannervik, B. (1991) Mutation of an evolutionarily conserved tyrosine residue in the active site of a human class Alpha glutathione transferase, *FEBS Lett. 293*, 153−155.
16. Wang, R. W., Newton, D. J., Huskey, S. E., McKeever, B. M., Pickett, C. B., and Lu, A. Y. (1992) Site-directed mutagenesis of glutathione S-transferase YaYa. Important roles of tyrosine 9 and aspartic acid 101 in catalysis, *J. Biol. Chem. 267*, 19866−19871.
17. Wang, J., Barycki, J. J., and Colman, R. F. (1996). Tyrosine 8 contributes to catalysis but is not required for activity of rat liver glutathione S-transferase, 1-1, *Protein Sci. 5*, 1032−1042.
18. Wang, R. W., Newton, D. J., Johnson, A. R., Pickett, C. B., and Lu, A. Y. (1993) Site-directed mutagenesis of glutathione S-transferase YaYa. Mapping the glutathione-binding site, *J. Biol. Chem. 268*, 23981−23985.
19. Bjornestedt, R., Stenberg, G., Widersten, M., Board, P. G., Sinning, I., Jones, T. A., and Mannervik, B. (1995) Functional significance of arginine 15 in the active site of human class alpha glutathione transferase A1-1, *J. Mol. Biol. 247*, 765−773.
20. Wang, R. W., Pickett, C. B., and Lu, A. Y. H. (1989) Expression of a cDNA encoding a rat liver glutathione S-transferase subunit in *Escherichia coli*, *Arch. Biochem. Biophys. 269*, 536−543.
21. Vargo, M. A., Nguyen, L., and Colman, R. F. (2004) Subunit interface residues of glutathione S-transferase A1-1 that are important in the monomer−dimer equilibrium, *Biochemistry 43*, 3327−3335.
22. Laemmli, U. K. (1970) Cleavage of structural proteins during the assembly of the head of bacteriophage T4, *Nature 227*, 680−685.
23. Katusz, R. M., Colman, R. F. (1991) S-(4-Bromo-2,3-dioxobutyl)-glutathione: a new affinity label for the 4-4 isoenzyme of rat liver glutathione S-transferase, *Biochemistry 30*, 11230−11238.
24. Habig, W. H., Pabst, M. J., and Jakoby, W. B. (1974) Glutathione S-transferases. The first enzymatic step in mercapturic acid formation, *J. Biol. Chem. 249*, 7130−7139.
25. Bradford, M. M. (1976) A rapid and sensitive method for the quantitation of microgram quantities of protein utilizing the principle of protein-dye binding, *Anal. Biochem. 72*, 248−254.
26. Cameron, A. D., Sinning, I., L'Hermite, G., Olin, B., Board, P. G., Mannervik, B., and Jones, T. A. (1995) Structural analysis of human alpha-class glutathione transferase A1-1 in the apo-form and in complexes with ethacrynic acid and its glutathione conjugate, *Structure 3*, 717−727.
27. Andrade, M. A., Chacon, P. Merelo, J. J., and Moran, F. (1993) Evaluation of secondary structure of proteins from UV circular dichroism spectra using an unsupervised learning neural network, *Protein Eng. 6*, 383−390.
28. Ricci, G., Del Boccio, G., Pennelli, A., Aceto, A., Whitehead E. P., and Federici, G. (1989) Nonequivalence of the two subunits of horse erythrocyte glutathione transferase in their reaction with sulfhydryl reagents, *J. Biol. Chem. 264*, 5462−5467.
29. Mao, L., Wang, Y., Liu, Y., and Hu, X. (2004) Molecular determinants for ATP-binding in proteins: a data mining and quantum chemical analysis, *J. Mol. Biol. 36*, 787−807.
30. Le Trong, I., Stenkamp, R. E., Ibarra, C., Atkins W. M., and Adman, E. T. (2002) 1.3 Å resolution structure of human

glutathione S-transferase with S-hexyl glutathione bound reveals possible extended ligandin binding site, *Proteins 48* (4), 618−627.
31. Mattos, C., and Ringe, D. (2001) Proteins in organic solvents, *Curr. Opin. Struct. Biol. 6*, 761−764.
32. Wallace, L. A., Sluis-Cremer, N., and Dirr, H. W. (1998) Equilibrium and Kinetic Unfolding Properties of Dimeric Human Glutathione Transferase A1-1, *Biochemistry 37*, 5320−5328.
33. Adman, E. T., Le Trong, I., Stenkamp, R. E., Nieslanik, B. S., Dietze, E. C., Tai, G., Ibarra, C., and Atkins, W. M. (2001) Localization of the C-terminus of rat glutathione S-transferase A1-1: crystal structure of mutants W21F and W21F/F220Y, *Proteins 42* (2), 192−200.
34. Nilsson, L. O., Edalat, M., Pettersson, P. L., and Mannervik, B. (2002) Aromatic residues in the C-terminal region of glutathione transferase A1-1 influence rate-determining steps in the catalytic mechanism, *Biochim. Biophys. Acta 1598*, 199−205.
35. Atkins, W. M., Dietze, E. C., Ibarra, C. (1997) Pressure-dependent ionization of Tyr9 in glutathione S-transferase A1-1: contribution of the C-terminal helix to a "soft" active site, *Protein Sci. 4*, 873−881.
36. Nieslanik, B. S., and Atkins, W. M. (2000) The catalytic Tyr-9 of glutathione S-transferase A1-1 controls the dynamics of the C terminus, *J. Biol. Chem. 275*, 17447−17451.

BI050449A